CHEMISTRY
A EUROPEAN JOURNAL

DOI: 10.1002/chem.200801645

All-Optical Integrated Logic Operations Based on Chemical Communication between Molecular Switches

Serena Silvi,[a] Edwin C. Constable,[c] Catherine E. Housecroft,[c] Jonathon E. Beves,[c] Emma L. Dunphy,[c] Massimiliano Tomasulo,[b] Françisco M. Raymo,*[b] and Alberto Credi*[a]

Abstract: Molecular logic gates process physical or chemical "inputs" to generate "outputs" based on a set of logical operators. We report the design and operation of a chemical ensemble in solution that behaves as integrated AND, OR, and XNOR gates with optical input and output signals. The ensemble is composed of a reversible merocyanine-type photoacid and a ruthenium polypyridine complex that functions as a pH-controlled three-state luminescent switch. The light-triggered release of protons from the photoacid is used to control the state of the transition-metal complex. Therefore, the two molecular switching devices communicate with one another through the exchange of ionic signals. By means of such a double (optical–chemical–optical) signal-transduction mechanism, inputs of violet light modulate a luminescence output in the red/far-red region of the visible spectrum. Nondestructive reading is guaranteed because the green light used for excitation in the photoluminescence experiments does not affect the state of the gate. The reset is thermally driven and, thus, does not involve the addition of chemicals and accumulation of byproducts. Owing to its reversibility and stability, this molecular device can afford many cycles of digital operation.

Keywords: luminescence · molecular devices · photochemistry · proton transfer · supramolecular chemistry

Introduction

The development of novel paradigms for information processing is the main motivation for investigating the implementation of molecular computing strategies. This alternative approach to silicon-based technology[1,2] could lead to the realization of computers of extremely small size, low power consumption, and unprecedented performance.[3] The rational basis for this research stems from the fact that, in living organisms, information is transported, elaborated, and stored by molecular or ionic substrates.[4–6] Although the components of a "molecular processor" will not necessarily have to operate in ways analogous to those of microelectronic circuits,[7] some efforts have been devoted to the design, synthesis, and characterization of chemical systems that mimic the operation of semiconductor logic gates and circuits.[8–26] Leaving aside futuristic speculations, systems of this kind could perform relatively simple computing tasks that cannot be accomplished with silicon-based devices, for example, the encoding[27] and networking[28] of microscopic objects, parallel chemical analyses in microfluidic systems,[29] control of the function of biomolecules,[30] and intelligent drug delivery in vitro[31,32] and in vivo.[33]

Molecular switches convert input stimulations into output signals,[34,35] and the principles of binary (Boolean) logic[36] can be applied to the signal transduction operated by molecules under appropriate conditions.[37] Implementation of the basic Boolean functions—PASS, YES, NOT, AND,

---

[a] Dr. S. Silvi, Prof. A. Credi
Dipartimento di Chimica "G. Ciamician"
Università di Bologna
via Selmi 2, 40126 Bologna (Italy)
Fax: (+39) 051-209-9456
E-mail: alberto.credi@unibo.it

[b] Dr. M. Tomasulo, Prof. F. M. Raymo
Center for Supramolecular Science, Department of Chemistry
University of Miami
1301 Memorial Drive, Coral Gables, FL 33146-0431 (USA)
Fax: (+1) 305-284-4571
E-mail: fraymo@miami.edu

[c] Prof. E. C. Constable, Prof. C. E. Housecroft, Dr. J. E. Beves,
Dr. E. L. Dunphy
Department of Chemistry
University of Basel
Spitalstrasse 51, 4056 Basel (Switzerland)

Supporting information for this article is available on the WWW under http://dx.doi.org/10.1002/chem.200801645.

NAND, OR, NOR, XOR, XNOR, INH—and the most common combinational circuits (for example, half- and full-adders and -subtractors, multiplexer, demultiplexer) with chemical systems has now been achieved.[8–26] Nevertheless, much remains to be done before the molecular logic approach will gain technological credibility. A critical issue of molecular logic gates is that, in most cases, the input and output signals have a different physical nature; this input/output inhomogeneity hinders the interconnection of basic elements to create complex circuits.[8,9,26b] In this regard, molecular logic devices that use optical input and output signals[15b,38–41] are particularly interesting[42] because 1) access for chemicals or wires is not required, 2) no waste products are formed on repeated cycling of the device, 3) operation in rigid or semirigid media is possible, and 4) the multichannel nature of light can be exploited to configure the device for different logic functions. Prototypical examples of this type of molecular logic gate based on the control of porphyrin fluorescence by covalently linked photochromic units have been reported.[9e,43]

Herein, we use a different approach to devise an all-optical molecular logic system that can perform simultaneously the two-input AND, OR, and XNOR logic functions. Our strategy is based on the coupled operation of two molecular switches, namely a photoacid that transduces optical inputs into ionic outputs (Sw1) and a three-state switch that responds to ionic inputs and provides optical outputs (Sw2; Scheme 1). The two switching units communicate with one another by chemical signals and are connected serially; that is, the photogenerated ionic output of Sw1 is the input of Sw2. We previously applied this strategy to photocontrol bistable acid–base switches to obtain simple light-driven molecular memories[44] and machines.[45] In the present work, we use light to access all of the states of a tristable acid–base switch, which allows us to implement nontrivial two-input logic functions. Additionally, we wish to develop the concept of *cascading* in molecular logic, whereby the output of an upstream switch constitutes the input for a downstream gate.[9,24,46] Very recently, it was shown that the exchange of chemical signals between distinct glass-supported monolayers of molecular switches by using a solution as the communication medium could be used to implement binary logic functions.[47] However, it should be noted that, until now, the serial connection of different molecular logic devices has been convincingly addressed only in the case of logic systems based on biomolecules[48] (enzymes[18,19b] or oligonucleotides[21,22,23c,d]).

The investigated compounds are shown in Scheme 1. Sw1 is based on a colorless spiropyran derivative, **SP**, which is converted into the yellow protonated merocyanine form, **ME**-H^+, in acid solution.[14a,49] On irradiation with visible light, **ME**-H^+ isomerizes back into **SP** and releases a proton into the solution (Scheme 1a). Sw2 is a $[Ru(tpy)_2]^{2+}$ complex (tpy = 2,2′:6′,2″-terpyridine) complex with 4-pyridyl substituents in the 4′-position of each tpy ligand.[50] In solution, this complex can exist in three different protonation states, namely, **Ru**$^{2+}$, **Ru**-H^{3+}, and **Ru**-H_2^{4+} (Scheme 1b). Spectroscopic titrations showed that these three forms 1) exhibit distinct and characteristic absorption spectra, luminescence spectra, and lifetimes (see the Supporting Information), 2) can be populated selectively, because the two pendant pyridyl units of **Ru**$^{2+}$ can be sequentially protonated in two consecutive steps, and 3) can be reversibly interconverted by stoichiometric additions of acid and base.[50] Therefore, **Ru**$^{2+}$ behaves as an acid–base-controlled three-state luminescent switch. As **SP** and **ME**-H^+ exhibit smaller and larger pK_a values than that of the pyridinium ion, respectively,[44b,45] we envisaged that the protonation state of the ruthenium complex could be controlled by light by using **ME**-H^+ as a photoacid.

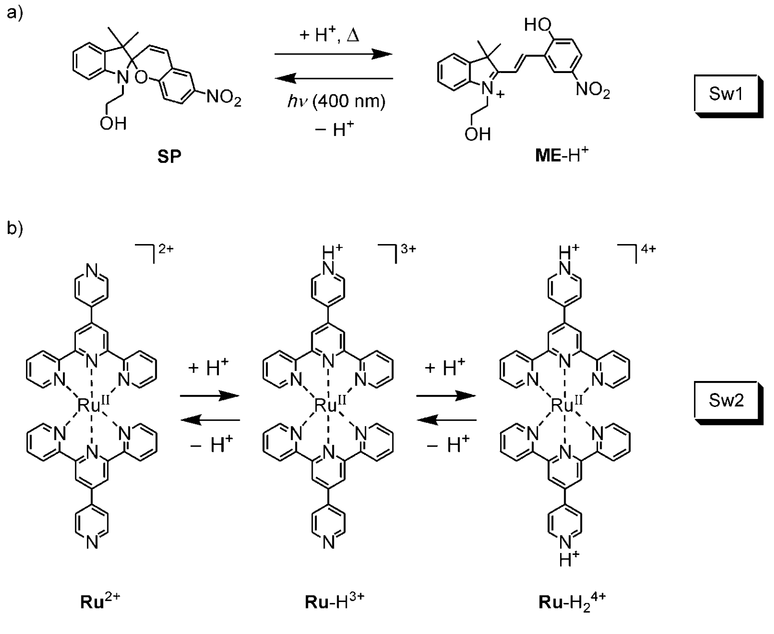

Scheme 1. Structure of the two molecular switches. a) Sw1: The acid- and light-controlled equilibrium between the spiropyran **SP** and the protonated merocyanine **ME**-H^+. b) Sw2: The acid–base-driven interconversion between the three protonation states of metal complex **Ru**$^{2+}$.

Results and Discussion

Photoinduced proton transfer between the molecular switches: The electronic absorption spectrum (Figure 1, solid line) of a newly prepared acetonitrile solution containing a 1:1 mixture of 1.6×10^{-5} M **Ru**-H^{3+} (obtained by addition of one equivalent of triflic acid to **Ru**$^{2+}$) and **SP** is essentially coincident with the sum of the

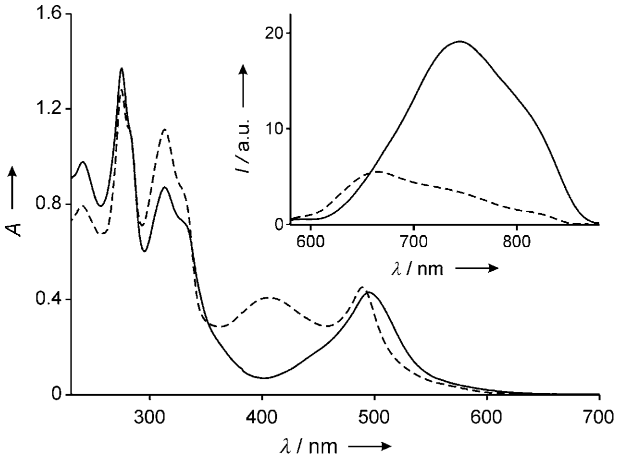

Figure 1. Absorption and (inset) luminescence spectra (CH_3CN, 293 K) of a newly prepared solution containing a 1:1 mixture of 1.6×10^{-5} M **Ru**-H^{3+} and **SP** (solid line). The dashed lines represent the spectra after 5 d in the dark at 293 K, at which point the solution contains **Ru**$^{2+}$ and **ME**-H^+. Upon exhaustive irradiation of the thermally equilibrated solution at 400 nm, the spectra represented by the solid lines are restored. For the luminescence spectra, excitation was performed at an isosbestic point at 493 nm.

spectra of the separate components. Specifically, the sharp and intense bands at $\lambda < 350$ nm are assigned to ligand-centered transitions of the metal complex, the shoulder in the 350–380 nm region is ascribed to the absorption of **SP**, and the band that peaks at 498 nm is the metal-to-ligand charge-transfer (MLCT) absorption band that is typical of **Ru**-H^{3+}. The luminescence spectrum (Figure 1, inset, solid line) shows a band with $\lambda_{max} = 737$ nm, which is assigned to emission from the triplet MLCT state of **Ru**-H^{3+}.[50] These features, however, change with time; after 5 d at 295 K (or 10 h at 318 K), no further changes occur and the absorption spectrum of the solution is that indicated by the dashed line in Figure 1. The blueshift of the visible MLCT band of the metal complex, which suggests that **Ru**$^{2+}$ is obtained,[50] and the appearance of a band that peaks at 401 nm, typical of **ME**-H^+,[49] indicate that the system has undergone an equilibration process that involves the transfer of a proton from the protonated metal complex to the photochrome. The luminescence spectral changes (Figure 1, inset) are consistent with the above observations: upon equilibration, the luminescence band of the metal complex decreases in intensity and shifts towards higher energy (dashed line), as expected with the transformation of **Ru**-H^{3+} into **Ru**$^{2+}$. From the analysis of the absorption and luminescence bands, it can be estimated that, at equilibrium, at least 90 % conversion into **Ru**$^{2+}$ and **ME**-H^+ occurs.

The absorption spectra reported in Figure 1 indicate that the **ME**-H^+ component can be photoexcited almost selectively in the spectral region around 400 nm and that exclusive excitation of the metal complex is possible at $\lambda >$ 480 nm, irrespective of its protonation state. Exhaustive irradiation of the solution at 400 nm (90 min under our conditions) leads to quantitative recovery of the initial absorption and luminescence spectra (see the Supporting Information), which indicates that 1) the **ME**-H^+ species has been photoconverted into **SP** and 2) the protonated complex **Ru**-H^{3+} has been regenerated. Leaving the solution for 5 d in the dark at 295 K (or 10 h at 318 K) leads once again to thermal equilibration and the formation of **Ru**$^{2+}$ and **ME**-H^+. Interestingly, switching between **Ru**$^{2+}$ and **Ru**-H^{3+} leads to a significant change in the emission intensity (Figure 1, inset), which indicates that, in this system, a red-luminescence signal can be modulated by a violet-light input. As noted above, the optical output reading can be performed with excitation at $\lambda > 480$ nm and, thus, it does not interfere with the switching process. It should also be noted that, because of the different intensity and spectral shape of the luminescence bands of **Ru**$^{2+}$ and **Ru**-H^{3+}, the emission intensity at, for example, 745 nm *increases* upon irradiation, whereas the intensity at, for example, 620 nm *decreases*. Several irradiation–equilibration cycles have been repeated on the same solution (Figure 2), and the results indicate that the off–on (620 nm) and on–off (745 nm) switching of luminescence is reversible.[51]

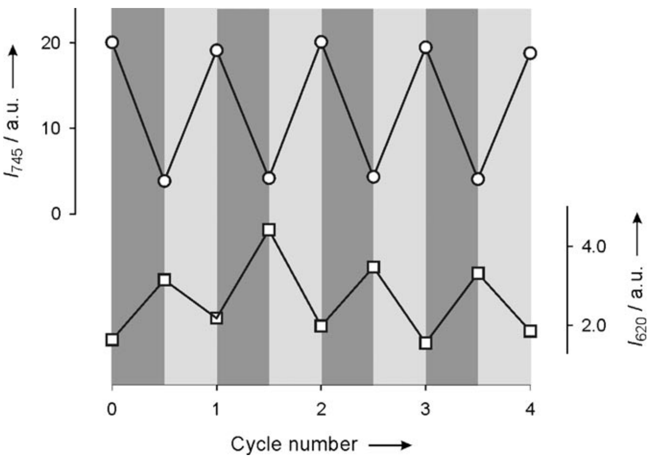

Figure 2. Emission-intensity values at 745 nm (○, left scale) and 620 nm (□, right scale) upon several equilibration–irradiation cycles performed on a solution containing a 1:1 mixture of 1.6×10^{-5} M **Ru**-H^{3+} and **SP**. Conditions: thermal equilibration (dark gray areas), 10 h in the dark at 318 K; light irradiation (light gray areas), 90 min at 400 nm.

The operation of the system is summarized by the thick lines in Figure 3. The initial, thermally equilibrated solution contains the photochrome in its open protonated form (**ME**-H^+) and the deprotonated complex (**Ru**$^{2+}$). Irradiation with violet light leads to isomerization of **ME**-H^+ into the closed form **SP** with concomitant release of a proton, which is taken up by the pendant pyridyl groups of the metal complex, and the protonated complex **Ru**-H^{3+} is formed. Such a photoproduced state evolves thermally in the dark to regenerate the initial thermodynamically stable system composed of **ME**-H^+ and **Ru**$^{2+}$. Overall, an optical input in the violet region (400 nm) is used to modulate an optical output in the red/far-red region (600–850 nm) as a result of intermolecular

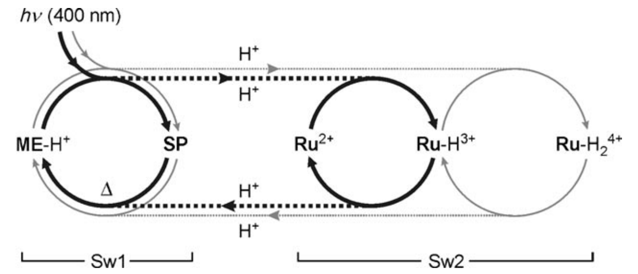

Figure 3. Coupled operation of the two-state switch Sw1 and three-state switch Sw2 by means of light-induced proton exchange. Irradiation of **ME**-H$^+$ such that one equivalent of protons is transferred to the metal complex generates the **Ru**-H$_3^+$ state (thick lines). Further irradiation of **ME**-H$^+$ can cause the transfer of another equivalent of protons to the metal complex, thereby generating the **Ru**-H$_2^{4+}$ state (thin lines). Subsequent thermal equilibration in the dark regenerates the initial state by reverse proton exchange.

communication of a chemical signal, represented by the transfer of protons.[44,45]

Photochemical three-state switching: To access all three states available for the metal complex, the photochemical cycle described above must be adapted such that the protonation of each of the basic pyridyl sites of the **Ru**$^{2+}$ species can be controlled. This issue can be tackled by mixing the photoacid and the metal complex in a 2:1 ratio and adjusting the dose of irradiating light to control the amount of protons—specifically, 1 or 2 equivalents with respect to **Ru**$^{2+}$—that are transferred from Sw1 to Sw2.

The absorption spectrum (Figure 4, dotted line) of an acetonitrile solution containing 2.4×10^{-5} M **Ru**-H$_2^{4+}$ (obtained by the addition of 2 equiv of triflic acid to **Ru**$^{2+}$) and 4.8×10^{-5} M **SP** is essentially coincident with the sum of the spectra of the separate **Ru**-H$_2^{4+}$ and **SP** components. The luminescence spectrum (Figure 5, dotted line) shows a band with $\lambda_{max}=729$ nm ($\tau=133$ ns), assigned to the **Ru**-H$_2^{4+}$ species.[50] After 5 d in the dark at 295 K (or 10 h at 318 K), both the absorption and emission spectra have changed (Figures 4 and 5, dashed lines). The blueshift and the intensity decrease of the visible MLCT absorption band of the metal complex and the appearance of an intense band that peaks at 401 nm indicate, respectively, that the **Ru**$^{2+}$ and **ME**-H$^+$ species are formed.[49,50] Hence, the system has undergone an equilibration process that involves the transfer of two H$^+$ ions from the protonated metal complex to the photochrome. The luminescence spectral changes (Figure 5) are consistent with the above observations: upon equilibration, the luminescence band of the metal complex decreases in intensity, as expected for the transformation of **Ru**-H$_2^{4+}$ into **Ru**$^{2+}$.[50] From the analysis of the absorption and luminescence bands, we estimate that, at equilibrium, 75 % of the metal complex exists as **Ru**$^{2+}$ and 25 % as **Ru**-H^{3+}, values that are in agreement with the amount of **ME**-H$^+$ formed (approximately 85 %). The luminescence decay shows a lifetime of 115 ns, which is fully consistent with the presence of **Ru**-H^{3+}.

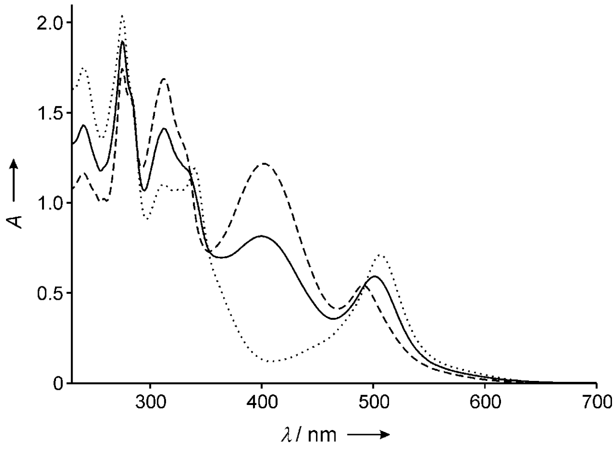

Figure 4. Absorption spectrum (CH$_3$CN, 293 K) of a newly prepared solution containing 2.4×10^{-5} M **Ru**-H$_2^{4+}$ and 4.8×10^{-5} mol L^{-1} **SP** (dotted line). The dashed line represents the spectrum after 5 d in the dark at 293 K, at which point the solution contains mostly **Ru**$^{2+}$ and **ME**-H$^+$. Upon partial irradiation (15 min) of the thermally equilibrated solution at 400 nm, the spectrum represented by the solid line is obtained, which indicates the formation of the **Ru**-H^{3+} species. Further exhaustive irradiation regenerates the initial spectrum (dotted line).

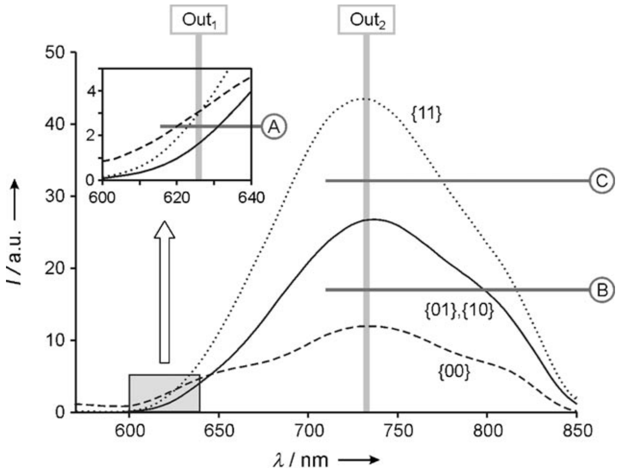

Figure 5. Luminescence spectrum (CH$_3$CN, 293 K, excitation at an isosbestic point at 493 nm) of a newly prepared solution containing 2.4×10^{-5} M **Ru**-H$_2^{4+}$ and 4.8×10^{-5} M **SP** (dotted line). The dashed line represents the spectrum after 5 d in the dark at 293 K, at which point the solution contains mostly **Ru**$^{2+}$ and **ME**-H$^+$. Upon partial irradiation (15 min) of the thermally equilibrated solution at 400 nm, the spectrum represented by the solid line is obtained, which is in agreement with the formation of the **Ru**-H^{3+} species. Further exhaustive irradiation regenerates the initial spectrum (dotted line). The inset shows a magnification of the 600–640 nm region. Input strings, output wavelengths (Out$_1$, Out$_2$), and threshold values (A, B, and C) relevant for the binary logic operations are indicated.

Exhaustive irradiation at 400 nm (120 min under our conditions) results in essentially complete recovery of the initial absorption and luminescence spectra (see the Supporting Information) and of the luminescence lifetime ($\tau=133$ ns), which indicates that 1) the **ME**-H$^+$ species has been photoconverted into **SP** and 2) the bis-protonated complex **Ru**-H_2^{4+} has been regenerated (Figure 3, thick and thin lines). After 5 d in the dark at 295 K (or 10 h at 318 K), the solution once again equilibrates with formation of $\mathbf{Ru}^{2+}$ and **ME**-H^+. Switching between $\mathbf{Ru}^{2+}$ and **Ru**-H_2^{4+} causes an even stronger change in the emission intensity (Figure 5) than in the previous case, in which the monoprotonated complex **Ru**-H^{3+} is obtained.

If the thermally equilibrated solution—composed of **ME**-H^+, $\mathbf{Ru}^{2+}$, and **Ru**-H^{3+} in a ratio of approximately 7:3:1 (see above)—is irradiated for only 15 minutes at 400 nm, the absorption and luminescence spectra indicated by the solid lines in Figures 4 and 5, respectively, are obtained. The decrease in the **ME**-H^+ absorbance at 401 nm, the change of the MLCT absorption band, and the redshift and intensity increase of the MLCT luminescence band of the metal complex, together with its lifetime ($\tau = 118$ ns), indicate that about 40 % of **ME**-H^+ has disappeared and monoprotonated **Ru**-H^{3+} has formed (see Figure 1 for comparison). These results are consistent with the transfer of one equivalent of H^+ ions from the photochrome to $\mathbf{Ru}^{2+}$, as shown by the thick lines in Figure 3. Further exhaustive irradiation (90 min under our conditions) of this solution at 400 nm causes spectral changes that indicate the complete disappearance of **ME**-H^+ and quantitative formation of **Ru**-H_2^{4+} (Figure 3, thin lines). The system is reset to the starting **ME**-H^+/$\mathbf{Ru}^{2+}$ state after 5 d in the dark at 295 K (or 10 h at 318 K). Hence, by controlling the amount of light absorbed by Sw1, all three protonation states of Sw2 can be reached.

The spectra reported in Figure 5 show that, for $\lambda >$ 650 nm, the emission intensity increases monotonically when 0, 1, and 2 equivalents of H^+ ions are transferred from Sw1 to Sw2. From a closer inspection of these spectra, however, it can be noticed that, in the region between 610 and 640 nm, the luminescence intensity decreases upon transfer of the first equivalent and increases upon transfer of the second equivalent.[51] This phenomenon implies that the luminescence intensity in this spectral region can decrease only if the dose of light irradiation does not overcome a certain threshold. As discussed in the previous section, this peculiar behavior is caused by the different shape and intensity of the luminescence bands exhibited by the metal complex in the three protonation states, and it has interesting consequences for the binary logic characteristics of the system.

Operation of the system as an all-optical integrated AND–OR–XNOR logic gate: This ruthenium complex, owing to the peculiar changes in its luminescence spectrum upon switching between the three differently protonated forms, can function as a photoionic molecular logic gate in which the two input signals are coded for by proton concentration and the output signal is provided by the luminescence intensity. On the other hand, in the previous sections, we have seen that the proton inputs for the $\mathbf{Ru}^{2+}$ switch can be photogenerated by dosing the amount of light absorbed by the **ME**-H^+ photoacid. Therefore, all-optical operation (writing and reading) of the logic gate is possible.

To digitally encode an (inherently analogue) physical or chemical signal and analyze the binary logic behavior of the system, an appropriate choice of the logic convention and threshold value must be made for each input and output channel. In this case, there are two input channels, represented by 400 nm light, to which a positive logic convention is applied. The input string {00} corresponds to dark conditions (no transfer of H^+ ions). The input strings {10} and {01} correspond to irradiation with the amount of 400 nm light needed to transfer one equivalent of protons from **ME**-H^+ to $\mathbf{Ru}^{2+}$ so that the complex **Ru**-H^{3+} is formed. It should be noted that the molecular system cannot distinguish between these input strings but the operator does, because the two light inputs can be supplied by two physically independent channels. The input string {11} corresponds to irradiation with a dose of 400 nm photons such that two equivalents of protons are transferred from **ME**-H^+ and the complex **Ru**-H_2^{4+} is obtained.

Figure 5 shows the luminescence spectra obtained upon excitation at an isosbestic point of 493 nm under conditions corresponding to the {00}, {01} or {10}, and {11} input strings. Three output channels with corresponding threshold values can be identified; a positive logic convention is adopted for all channels. If threshold A is applied and the luminescence intensity at 626 nm is taken as the output signal (Out_1),[51] the logic behavior is that of an XNOR gate (Table 1). By taking the luminescence intensity at 732 nm as the output signal (Out_2), the OR function is obtained if threshold B is applied, whereas the logic behavior is that of an AND gate with adoption of threshold C. Hence, the same molecular system integrates three fundamental logic operations (Table 1) by taking advantage of different output channels and appropriate logic threshold values. Figure 6 shows a plot of the luminescence intensity values of the two outputs for consecutive switching cycles on the same solution. These results demonstrate that the switching process is reversible and that the signal-to-noise ratio is largely sufficient to afford an error-free digital operation of the gate for several cycles. It is worth noting that if a negative logic convention is adopted for Out_1, the XOR function is obtained; its combination with the AND function (Out_3) gives rise to the truth table of the half-adder operation.[8,9,40]

Table 1. Truth table for the XNOR, OR, and AND logic behavior of the investigated molecular logic device.

In_1[a] $\lambda_{irr} = 400$ nm	In_2[a] $\lambda_{irr} = 400$ nm	Out_1[b] $\lambda_{em} = 626$ nm threshold A XNOR gate	Out_2[b] $\lambda_{em} = 732$ nm threshold B OR gate	threshold C AND gate
0	0	1	0	0
0	1	0	1	0
1	0	0	1	0
1	1	1	1	1

[a] Positive logic convention; digital "1" corresponds to irradiation with the amount of 400 nm light needed to generate one equivalent of protons with respect to the metal complex. [b] Positive logic convention; the actual values of the luminescence intensities and thresholds are indicated in Figures 5 and 6.

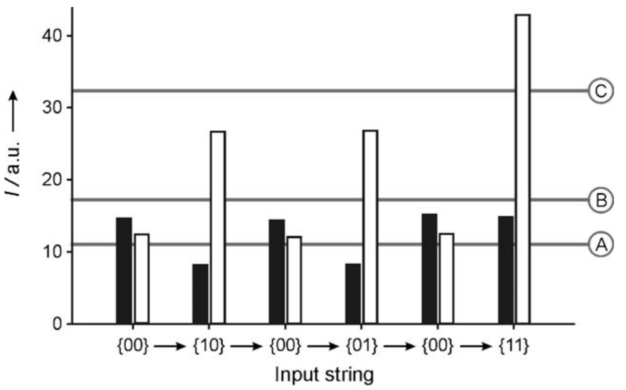

Figure 6. Response of the device to different input strings and cycling. Shaded and white bars represent the experimental luminescence intensities at 626 nm (Out_1) and 732 nm (Out_2), respectively. The intensity values at 626 nm have been multiplied by five for the sake of clarity. Marks A, B, and C represent the threshold values for the XNOR, OR, and AND operations, respectively (see Table 1). The experimental conditions are those described for Figure 5. Input conditions: {00}, 10 h at 318 K; {10} and {01}, irradiation at 400 nm for 15 minutes; {11}, exhaustive irradiation at 400 nm.

The set of logic functions available to this system can be further expanded if other chemical inputs, such as dioxygen, are used. Moreover, the large difference between the timescales of the light-irradiation and thermal-equilibration processes can be exploited to implement the memory-effect characteristic of sequential logic circuits.[44]

Conclusion

The coupled operation of the acid–base switchable complex **Ru**$^{2+}$ and the photochromic pair **SP**/**ME**-H$^+$ has allowed us to devise a chemical system that integrates AND, OR, and XNOR logic operations in which both the input and output signals are optical. Owing to its reversibility and stability, the molecular logic device can be cycled several times while maintaining a satisfactory signal-to-noise ratio.

We would like to emphasize that the purpose of this work was to study the feasibility of a strategy based on chemically communicating molecular switches for achieving the desired functionalities, not to investigate practically useful applications. Such an approach is interesting because it is reminiscent of information processing and transfer in living organisms.[4,5] In fact, our results demonstrate that communication of chemical signals can be employed to co-operate distinct molecular logic gates.[47] Experiments of this kind may be viewed as a first simple step towards *cascading*—in which the output of an upstream gate constitutes the input for a downstream gate—in logic devices based on fully artificial molecules.[48] Certainly, the fact that the system relies on diffusion of ions in a fluid solution poses limitations to its technological appeal, although it is well known that intermolecular proton-transfer processes are also possible in solid matrices.[52] Moreover, the slow switching time alone would be a serious drawback in most applicative contexts.

Nevertheless, our molecular logic device possesses a number of interesting features that are not found together in other reported systems: 1) all input and output signals are coded for by visible light, 2) the outputs correspond to wavelengths in a spectral region (red/far red) that is interesting, for instance, in communication technology[53] and diagnostics,[54] 3) the photoluminescence output reading has no effect on the state of the gate (nondestructive reading), and 4) the reset process is thermally driven and, thus, does not involve the addition of chemicals and accumulation of byproducts.

Experimental Section

Synthesis: The syntheses of **SP** and **Ru**$^{2+}$ have been previously reported.[49,50,55] Triflic acid (CF_3SO_3H) was purchased from Fluka and used as received.

Absorption and luminescence experiments: The absorption and luminescence spectra were recorded with a Perkin–Elmer λ40 spectrophotometer and a Perkin–Elmer LS-50 spectrofluorimeter equipped with a Hamamatsu R928 photomultiplier. Air-equilibrated acetonitrile (Merck Uvasol) solutions with concentrations ranging from 1×10^{-5} to 1×10^{-4} M were examined in 1 cm spectrofluorimetric quartz cells at 293 K. Luminescence spectra were recorded upon excitation at isosbestic points and were not corrected for the monochromator–detector spectral response. Luminescence-lifetime measurements were carried out with a Proteus flash photolysis spectrometer (Ultrafast Systems) by exciting the sample with 10 ns (full width at mid height) pulses of a Continuum Surelite I-10 Nd/YAG laser. Excitation was performed at $\lambda = 532$ nm, obtained by frequency doubling. The light was detected by a Hamamatsu R928 photomultiplier and recorded on a Tektronix TDS 3032 B (300 MHz) digital oscilloscope connected to a personal computer. Each decay was obtained by averaging 64 pulses. The experimental error on the wavelength values was ±1 nm, and the errors on the absorbance, luminescence intensity, and lifetime values were estimated to be ±5%.

Photochemical experiments: Irradiation experiments were carried out by using the Xe arc lamp monochromator ensemble of a Perkin–Elmer LS-50 spectrofluorimeter. The light intensity at 400 nm, measured by ferrioxalate actinometry, was 5×10^{-9} Einstein min^{-1} on a 3 mL volume.

Acknowledgements

This work was supported by the U.S. National Science Foundation (CAREER Award CHE-0237578 and CHE-0749840), the Swiss National Science Foundation, and, in Italy, by the Ministero dell'Università e della Ricerca, Regione Emilia-Romagna, and the Università di Bologna. E.C.C. thanks the Swiss Nanoscience Institute and National Center of Competence in Research "Nanoscale Science" for support.

---

[1] *ITRS Roadmap for Semiconductors*, *2007 Edition*, available at http://www.itrs.net (accessed August 2008).

[2] R. Chau, B. Doyle, S. Datta, J. Kavalieros, K. Zhang, *Nat. Mater.* **2007**, *6*, 810–812.

[3] J. E. Green, J. W. Choi, A. Boukai, Y. Bunimovich, E. Johnston-Halperin, E. DeIonno, Y. Luo, B. A. Sheriff, K. Xu, Y. S. Shin, H.-R. Tseng, J. F. Stoddart, J. R. Heath, *Nature* **2007**, *445*, 414–417.

[4] D. S. Goodsell, *Bionanotechnology—Lessons from Nature*, Wiley, New York, **2004**.

[5] R. Ballardini, P. Ceroni, A. Credi, M. T. Gandolfi, M. Maestri, M. Semeraro, M. Venturi, V. Balzani, *Adv. Funct. Mater.* **2007**, *17*, 740–750.

[6] J.-M. Lehn, *Proc. Natl. Acad. Sci. USA* **2002**, *99*, 4763–4768.

[7] A. Tullo, *Chem. Eng. News* **2006**, *84*(35), 22.

[8] V. Balzani, A. Credi, M. Venturi, *Molecular Devices and Machines—Concepts and Perspectives for the Nanoworld*, 2nd ed., Wiley-VCH, Weinheim, **2008**, Chapter 9.

[9] a) F. M. Raymo, *Adv. Mater.* **2002**, *14*, 401–414; b) V. Balzani, A. Credi, M. Venturi, *ChemPhysChem* **2003**, *4*, 49–59; c) P. M. Mendes, A. H. Flood, J. F. Stoddart, *Appl. Phys. A* **2005**, *80*, 1197–1209; d) A. P. de Silva, *Nat. Mater.* **2005**, *4*, 15–16; e) D. Gust, T. A. Moore, A. L. Moore, *Chem. Commun.* **2006**, 1169–1178; f) A. P. de Silva, S. Uchiyama, *Nat. Nanotechnol.* **2007**, *2*, 399–410; g) A. Credi, *Angew. Chem.* **2007**, *119*, 5568–5572; *Angew. Chem. Int. Ed.* **2007**, *46*, 5472–5475; h) U. Pischel, *Angew. Chem.* **2007**, *119*, 4100–4115; *Angew. Chem. Int. Ed.* **2007**, *46*, 4026–4040; i) K. Szaciłowski, *Chem. Rev.* **2008**, *108*, 3481–3548.

[10] a) A. P. de Silva, N. D. McClenaghan, *Chem. Eur. J.* **2004**, *10*, 574–586; b) S. Uchiyama, D. D. McClean, K. Iwai, A. P. de Silva, *J. Am. Chem. Soc.* **2005**, *127*, 8920–8921; c) D. C. Magri, G. J. Brown, G. D. McClean, A. P. de Silva, *J. Am. Chem. Soc.* **2006**, *128*, 4950–4951; d) A. P. de Silva, Y. Leydet, C. Lincheneau, N. D. McClenaghan, *J. Phys. Condens. Matter* **2006**, *18*, S1847–S1872; e) A. P. de Silva, S. S. K. de Silva, N. C. W. Goonesekera, H. Q. N. Gunaratne, P. L. M. Lynch, K. R. Nesbitt, S. T. Patuwathavithana, N. L. D. S. Ramyalal, *J. Am. Chem. Soc.* **2007**, *129*, 3050–3051.

[11] a) S. J. Langford, T. Yann, *J. Am. Chem. Soc.* **2003**, *125*, 11198–11199; b) S. J. Langford, T. Yann, *J. Am. Chem. Soc.* **2003**, *125*, 14951.

[12] a) D. Margulies, G. Melman, A. Shanzer, *Nat. Mater.* **2005**, *4*, 768–771; b) D. Margulies, G. Melman, A. Shanzer, *J. Am. Chem. Soc.* **2006**, *128*, 4865–4871; c) D. Margulies, C. E. Felder, G. Melman, A. Shanzer, *J. Am. Chem. Soc.* **2007**, *129*, 347–354.

[13] a) K. Szaciłowski, *Chem. Eur. J.* **2004**, *10*, 2520–2528; b) K. Szaciłowski, W. Macyk, G. Stochel, *J. Am. Chem. Soc.* **2006**, *128*, 4550–4551; c) W. Macyk, G. Stochel, K. Szaciłowski, *Chem. Eur. J.* **2007**, *13*, 5676–5687.

[14] a) F. M. Raymo, S. Giordani, *J. Am. Chem. Soc.* **2001**, *123*, 4651–4652; b) F. M. Raymo, M. Tomasulo, *Chem. Eur. J.* **2006**, *12*, 3186–3193; c) S. Sortino, S. Petralia, S. Di Bella, M. Tomasulo, F. M. Raymo, *New J. Chem.* **2006**, *30*, 515–517.

[15] a) F. Remacle, S. Speiser, R. D. Levine, *J. Phys. Chem. B* **2001**, *105*, 5589–5591; b) F. Remacle, R. D. Levine, *Phys. Rev. A* **2006**, *73*, 033820; c) F. Remacle, R. Weinkauf, R. D. Levine, *J. Phys. Chem. A* **2006**, *110*, 177–184.

[16] a) H. T. Baytekin, E. U. Akkaya, *Org. Lett.* **2000**, *2*, 1725–1727; b) A. Coskun, E. Deniz, E. U. Akkaya, *Org. Lett.* **2005**, *7*, 5187–5189.

[17] K. Rurack, C. Trieflinger, A. Koval'chuck, J. Daub, *Chem. Eur. J.* **2007**, *13*, 8998–9003.

[18] a) R. Baron, O. Lioubashevski, E. Katz, T. Niazov, I. Willner, *Angew. Chem.* **2006**, *118*, 1602–1606; *Angew. Chem. Int. Ed.* **2006**, *45*, 1572–1576; b) R. Baron, O. Lioubashevski, E. Katz, T. Niazov, I. Willner, *J. Phys. Chem. A* **2006**, *110*, 8548–8553; c) T. Niazov, R. Baron, E. Katz, O. Lioubashevski, I. Willner, *Proc. Natl. Acad. Sci. USA* **2006**, *103*, 17160–17163.

[19] a) M. Pita, E. Katz, *J. Am. Chem. Soc.* **2008**, *130*, 36–37; b) G. Strack, M. Ornatska, M. Pita, E. Katz, *J. Am. Chem. Soc.* **2008**, *130*, 4234–4235.

[20] a) D. H. Qu, Q. C. Wang, H. Tian, *Angew. Chem.* **2005**, *117*, 5430–5433; *Angew. Chem. Int. Ed.* **2005**, *44*, 5296–5299; b) Z. Q. Guo, W. H. Zhu, L. J. Shen, H. Tian, *Angew. Chem.* **2007**, *119*, 5645–5649; *Angew. Chem. Int. Ed.* **2007**, *46*, 5549–5553; c) Z. Q. Guo, P. Zhao, W. H. Zhu, X. M. Huang, Y. S. Xie, H. Tian, *J. Phys. Chem. C* **2008**, *112*, 7047–7053; d) H. Tian, Y. L. Feng, *J. Mater. Chem.* **2008**, *18*, 1617–1622.

[21] a) M. N. Stojanovic, T. E. Mitchell, D. Stefanovic, *J. Am. Chem. Soc.* **2002**, *124*, 3555–3561; b) M. N. Stojanovic, S. Semova, D. Kolpashchikov, J. Macdonald, C. Morgan, D. Stefanovic, *J. Am. Chem. Soc.* **2005**, *127*, 6914–6915; c) J. Macdonald, Y. Li, M. Sutovic, H. Lederman, K. Pendri, W. Lu, B. L. Andrews, D. Stefanovic, M. N. Stojanovic, *Nano Lett.* **2006**, *6*, 2598–2603; d) H. Lederman, J. Macdonald, D. Stefanovic, M. N. Stojanovic, *Biochemistry* **2006**, *45*, 1194–1199.

[22] a) G. Seelig, D. Soloveichnik, D. Y. Zhang, E. Winfree, *Science* **2006**, *314*, 1585–1588; b) D. Y. Zhang, A. J. Turberfield, B. Yurke, E. Winfree, *Science* **2007**, *318*, 1121–1125.

[23] a) G. Ashkenasy, M. R. Ghadiri, *J. Am. Chem. Soc.* **2004**, *126*, 11140–11141; b) N. C. Gianneschi, M. R. Ghadiri, *Angew. Chem.* **2007**, *119*, 4029–4032; *Angew. Chem. Int. Ed.* **2007**, *46*, 3955–3958; c) B. M. Frezza, S. L. Cockroft, M. R. Ghadiri, *J. Am. Chem. Soc.* **2007**, *129*, 14875–14879; d) N. H. Voelcker, K. M. Guckian, A. Saghatelian, M. R. Ghadiri, *Small* **2008**, *4*, 427–431.

[24] U. Pischel, B. Heller, *New J. Chem.* **2008**, *32*, 395–400.

[25] E. Perez-Inestrosa, J.-M. Montenegro, D. Collado, R. Suau, *Chem. Commun.* **2008**, 1085–1087.

[26] a) A. Credi, V. Balzani, S. J. Langford, J. F. Stoddart, *J. Am. Chem. Soc.* **1997**, *119*, 2679–2681; b) M. Amelia, M. Baroncini, A. Credi, *Angew. Chem.* **2008**, *120*, 6336–6339; *Angew. Chem. Int. Ed.* **2008**, *47*, 6240–6243.

[27] A. P. de Silva, D. Y. James, B. O. F. McKinney, D. A. Pears, S. M. Weir, *Nat. Mater.* **2006**, *5*, 787–790.

[28] a) G. von Maltzahn, T. J. Harris, J.-H. Park, D.-H. Min, A. J. Schmidt, M. J. Sailor, S. N. Bhatia, *J. Am. Chem. Soc.* **2007**, *129*, 6064–6065; b) R. Yashin, S. Rudchenko, M. N. Stojanovic, *J. Am. Chem. Soc.* **2007**, *129*, 15581–15584.

[29] S. Kou, H. N. Lee, D. van Noort, K. M. K. Swamy, S. H. Kim, J. H. Soh, K.-M. Lee, S.-W. Nam, J. Yoon, S. Park, *Angew. Chem.* **2008**, *120*, 886–890; *Angew. Chem. Int. Ed.* **2008**, *47*, 872–876.

[30] S. Muramatsu, K. Kinbara, H. Taguchi, N. Ishii, T. Aida, *J. Am. Chem. Soc.* **2006**, *128*, 3764–3769.

[31] R. J. Amir, M. Popkov, R. A. Lerner, C. F. Barbas III, D. Shabat, *Angew. Chem.* **2005**, *117*, 4452–4455; *Angew. Chem. Int. Ed.* **2005**, *44*, 4378–4381.

[32] a) Y. Benenson, B. Gil, U. Ben-Dor, R. Adar, E. Shapiro, *Nature* **2004**, *429*, 423–429; b) E. Shapiro, B. Gil, *Nat. Nanotechnol.* **2007**, *2*, 84–85.

[33] K. Rinaudo, L. Bleris, R. Maddamsetti, S. Subramanian, R. Weiss, Y. Benenson, *Nat. Biotechnol.* **2007**, *25*, 795–801.

[34] *Molecular Switches*, 2nd ed. (Ed.: B. L. Feringa), Wiley-VCH, Weinheim, **2008**.

[35] V. Balzani, A. Credi, M. Venturi, *Chem. Eur. J.* **2008**, *14*, 26–39.

[36] J. R. Gregg, *Ones and Zeros: Understanding Boolean Algebra, Digital Circuits, and the Logic of Sets*, Wiley, New York, **1998**.

[37] For the first experimental demonstration of the analogy between molecular switches and logic gates, see: A. P. de Silva, H. Q. N. Gunaratne, C. P. McCoy, *Nature* **1993**, *364*, 42–44.

[38] A. S. Lukas, P. J. Bushhard, M. R. Wasielewski, *J. Am. Chem. Soc.* **2001**, *123*, 2440–2441.

[39] F. M. Raymo, S. Giordani, *Proc. Natl. Acad. Sci. USA* **2002**, *99*, 4941–4944.

[40] J. Andréasson, S. D. Straight, G. Kodis, C.-D. Park, M. Hambourger, M. Gervaldo, B. Albinsson, T. A. Moore, A. L. Moore, D. Gust, *J. Am. Chem. Soc.* **2006**, *128*, 16259–16265.

[41] O. Kuznetz, H. Salman, N. Shakkour, Y. Eichen, S. Speiser, *Chem. Phys. Lett.* **2008**, *451*, 63–67.

[42] It is worth noting that, in the case of all-optical molecular logic gates, thermodynamically downhill energy-transfer processes are required to achieve serial connection. Hence, only a limited number of serial integrations can be performed before the energy of the photons used to propagate the signal becomes too small. For a brief discussion, see reference [15a].

[43] a) S. D. Straight, J. Andréasson, G. Kodis, S. Bandyopadhyay, R. H. Mitchell, T. A. Moore, A. L. Moore, D. Gust, *J. Am. Chem. Soc.* **2005**, *127*, 9403–9409; b) S. D. Straight, P. A. Liddell, Y. Terazono, T. A. Moore, A. L. Moore, D. Gust, *Adv. Funct. Mater.* **2007**, *17*, 777–785; c) J. Andréasson, S. D. Straight, S. Bandyopadhyay, R. H. Mitchell, T. A. Moore, A. L. Moore, D. Gust, *Angew. Chem.* **2007**, *119*, 976–979; *Angew. Chem. Int. Ed.* **2007**, *46*, 958–961; d) J. Andreasson, S. D. Straight, S. Bandyopadhyay, R. H. Mitchell, T. A.

Moore, A. L. Moore, D. Gust, *J. Phys. Chem. C* **2007**, *111*, 14274–14278.

[44] a) F. M. Raymo, S. Giordani, *Org. Lett.* **2001**, *3*, 3475–3478; b) F. M. Raymo, R. J. Alvarado, S. Giordani, M. A. Cejas, *J. Am. Chem. Soc.* **2003**, *125*, 2361–2364; c) S. Giordani, M. A. Cejas, F. M. Raymo, *Tetrahedron* **2004**, *60*, 10973–10981.

[45] S. Silvi, A. Arduini, A. Pochini, A. Secchi, M. Tomasulo, F. M. Raymo, M. Baroncini, A. Credi, *J. Am. Chem. Soc.* **2007**, *129*, 13378–13379.

[46] A. Credi, *Nat. Nanotechnol.* **2008**, *3*, 529–530.

[47] a) T. Gupta, M. E. van der Boom, *Angew. Chem.* **2008**, *120*, 2292–2294; *Angew. Chem. Int. Ed.* **2008**, *47*, 2260–2262; b) T. Gupta, M. E. van der Boom, *Angew. Chem.* **2008**, *120*, 5402–5406; *Angew. Chem. Int. Ed.* **2008**, *47*, 5322–5325.

[48] It should be recalled that, although the oligonucleotides used in references [21], [22], and [23c,d] are synthetic molecules, their operation as logic devices relies on the outstanding recognition properties of the natural DNA bases.

[49] F. M. Raymo, S. Giordani, A. J. P. White, D. J. Williams, *J. Org. Chem.* **2003**, *68*, 4158–4169.

[50] E. C. Constable, C. E. Housecroft, A. Cargill Thompson, P. Passaniti, S. Silvi, M. Maestri, A. Credi, *Inorg. Chim. Acta* **2007**, *360*, 1102–1110.

[51] The emission intensity changes in the region between 610 and 640 nm upon protonation of the **Ru**$^{2+}$ species, albeit small, are easily detectable with a standard spectrofluorimeter and are fully reproducible; see Figure 2, Figure 6, and the Supporting Information.

[52] S. Giordani, F. M. Raymo, *Org. Lett.* **2003**, *5*, 3559–3562.

[53] J. H. Franz, V. K. Jain, *Optical Communications: Components and Systems*, CRC Press, Boca Raton, **2000**.

[54] B. R. Masters, *Confocal Microscopy and Multiphoton Excitation Microscopy: The Genesis of Live Cell Imaging*, SPIE, Bellingham, **2006**.

[55] J. E. Beves, E. L. Dunphy, E. C. Constable, C. E. Housecroft, C. J. Kepert, M. Neuburger, D. J. Price, S. Schaffner, *Dalton Trans.* **2008**, 386–396.

Received: August 8, 2008